

# <sup>13</sup>C NMR Relaxation Rates in the Ionic Liquid 1-Ethyl-3-methylimidazolium Butanesulfonate

Norman E. Heimer,<sup>‡</sup> John S. Wilkes,<sup>‡</sup> Phillip G. Wahlbeck,<sup>†</sup> and W. Robert Carper<sup>\*,‡,†</sup>

Department of Chemistry, USAF Academy, Colorado 80840-6230, and Department of Chemistry, Wichita State University, Wichita, Kansas 67260-0051

Received: October 21, 2005; In Final Form: November 14, 2005

A new method of obtaining molecular reorientational dynamics from <sup>13</sup>C spin–lattice relaxation data of aromatic carbons in viscous solutions is applied to <sup>13</sup>C relaxation data of both the cation and anion in the ionic liquid, 1-ethyl-3-methylimidazolium butanesulfonate ([EMIM]BSO<sub>3</sub>). <sup>13</sup>C pseudorotational correlation times are used to calculate corrected maximum NOE factors from a combined isotropic dipolar and nuclear Overhauser effect (NOE) equation. These corrected maximum NOE factors are then used to determine the dipolar relaxation rate part of the total relaxation rate for each aromatic <sup>13</sup>C nucleus in the imidazolium ring. Rotational correlation times are compared with viscosity data and indicate several [EMIM]BSO<sub>3</sub> phase changes over the temperature range from 278 to 328 K. Modifications of the Stokes–Einstein–Debye (SED) model are used to determine molecular radii for the 1-ethyl-3-methylimidazolium cation. The Hu–Zwanzig correction yields a cationic radius that compares favorably with a DFT gas-phase calculation, B3LYP/(6-311+G(2d,p)). Chemical shift anisotropy values, Δσ, are obtained for the ring and immediately adjacent methylene and methyl carbons in the imidazolium cation and for the three carbon atoms nearest to the sulfonate group in the anion.

## Introduction

Room-temperature ionic liquids (RTILs) have generated considerable excitement in recent years as a new type of solvent media that possesses minimal vapor pressure.<sup>1–5</sup> Ionic liquids can be recycled, thus making synthetic processes less expensive and potentially more efficient and environmentally friendly. As a result, the interest in ionic liquids as a reaction media has intensified in recent years and has resulted in the reporting of many new ionic liquids including those that contain both organic cations and organic anions such as the sulfates<sup>6–10</sup> and sulfonates.<sup>11,12</sup>

The ability of ionic liquids to form supramolecular aggregates has always been suspected by various investigators and recent reports in the literature establish this as factual using mass spectrophotometric, <sup>1</sup>H NMR, conductivity and microcalorimetric methods.<sup>13,14</sup> The ability of room temperature ionic liquids to aggregate undoubtedly affects their ability to serve as efficient reaction media and suggests that those methods identifying the aggregations process may prove to be quite useful.

In particular, nuclear relaxation rates often provide valuable information concerning the dynamics and molecular interactions that occur in the liquid state.<sup>15–31</sup> Use of nuclear spin–lattice relaxation rates to obtain information concerning reorientational dynamics is often restricted to the extreme narrowing region. In this region, the product of the resonance frequency and the rotational correlation time is less than unity. However, many ionic liquid systems of interest are viscous such that one is outside of the region of extreme narrowing and relaxation rates are frequency dependent. The rotational correlation equations that describe the frequency-dependent region are considerably more complex and analysis is somewhat more difficult.

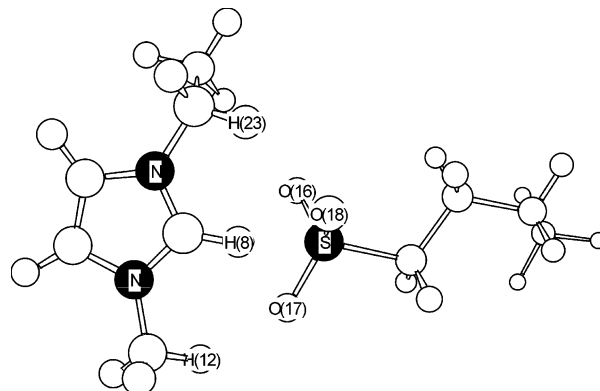


**Figure 1.** DFT (gas phase) molecular structure of [EMIM]BSO<sub>3</sub> (B3LYP/6-311+G(2d,p)). Hydrogen bonds include O18–H23 = 2.542 Å, O18–H8 = 1.929 Å, O17–H8 = 2.492 Å and O17–H12 = 2.235 Å.

In this <sup>13</sup>C NMR relaxation and viscosity study, a relatively new method of <sup>13</sup>C NMR relaxation analysis is applied to both the cation and anion of the 1-ethyl-3-methylimidazolium butanesulfonate ([EMIM]BSO<sub>3</sub>) ionic liquid shown in Figure 1.<sup>30,31</sup> This method has been used previously in <sup>13</sup>C NMR studies of the 1-butyl-3-methylimidazolium hexafluorophosphate ([BMIM]PF<sub>6</sub>) and 1-methyl-3-nonylimidazolium hexafluorophosphate ([NMIM]PF<sub>6</sub>) ionic liquids.<sup>30,31</sup>

The [EMIM]BSO<sub>3</sub> <sup>13</sup>C relaxation data reported herein is correlated with viscosity data obtained for the same ionic liquid, and indicates several phase changes for both the 1-ethyl-3-methylimidazolium cation and the butanesulfonate anion. The ability to analyze both cationic and anionic molecular dynamics using the same physical method is potentially a very useful technique.

## Experimental Section

### Materials: 1-Ethyl-3-methylimidazolium Butanesulfonate.

Equimolar quantities of 1-ethyl-3-methylimidazolium chloride,

\* Corresponding author. E-mail: Bob.Carper@wichita.edu.

<sup>‡</sup> USAF Academy.

<sup>†</sup> Wichita State University.

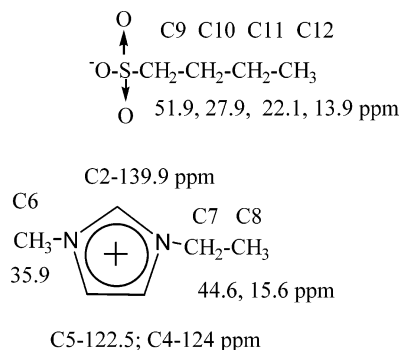


**Figure 2.** Chemical shift values (<sup>13</sup>C, ppm) and carbon positions for the 1-ethyl-3-methylimidazolium butyl sulfate ionic liquid.

locally prepared, and sodium butanesulfonate, Lancaster Synthesis Inc., were mixed as solids and allowed to stand at room temperature for 1 week. During this time a liquid appeared above a colorless solid. The ionic liquid was separated from the NaCl present by dissolution in 5 mL of acetonitrile for each gram of total reactants in the preparation followed by carefully decanting the acetonitrile solution from the insoluble salt. This was repeated two more times and most of the acetonitrile was removed using a rotary evaporator. The clear viscous liquid that remained was dried for 3 days under vacuum, 0.1 Torr removing all but a trace of water as seen from the IR spectrum: IR (NaCl, cm<sup>-1</sup>) 3464, 3146, 3094, 2960, 2872, 1563, 1467, 1277, 1234, 1190, 1037, 783, 720, 650, 624, 610; <sup>1</sup>H NMR (neat liquid in a sealed capillary immersed in CDCl<sub>3</sub>, 25 °C, δ) 9.54, 8.08, 7.96, 4.32 (q), 4.01, 2.50 (t), 1.52 (broad envelope), 1.36 (t), 1.23 (q), 0.71 (t); <sup>13</sup>C NMR (neat liquid in a sealed capillary immersed in CDCl<sub>3</sub>, 25 °C, δ) 139.9, 124.0, 122.5, 51.9, 44.6, 35.9, 27.9, 22.1, 15.6, 13.9. The resulting ionic liquid is insoluble in ether or hexanes but is readily soluble in water.

**Viscosity Measurements.** Viscosity measurements were made using a Viscolab 4100 moving piston Viscosity Monitoring and Control Electronics System. Temperature control was provided by a VWR Programmable Temperature Controller, Model 1167. The reported values are averages of about 20 measurements and estimates of the reproducibility of the measurements are ±0.1%. Temperature changes during the viscosity measurement were less than ±0.1°.

**Computational Methods.** B3LYP calculations using the (6-311+G(2d,p)) basis set were obtained using GAUSSIAN 98.<sup>32</sup> As an internal check, vibrational analyses on [EMIM]BSO<sub>3</sub> (Figure 1) revealed a lack of imaginary frequencies, ensuring the presence of a true minimum. Molecular volumes were calculated under tight convergence to reduce error. Hydrogen bonds (Figure 1) are defined as those interatomic distances less than the sum of the van der Waals radii.<sup>33,34</sup>

**NMR Relaxation Measurements.** The <sup>13</sup>C NMR relaxation data were measured on a Varian Unity-Plus spectrometer using a D<sub>2</sub>O capillary for a lock. (*B*<sub>0</sub> = 4.70 T, *v*<sub>0</sub>(<sup>13</sup>C) = 50.31 MHz, *v*<sub>0</sub>(<sup>1</sup>H) = 200.10 MHz. The δ<sub>C</sub> chemical shift assignments for [EMIM]BSO<sub>3</sub> are shown in Figure 2.

The spin–lattice relaxation times were measured using the inversion–recovery pulse sequence and calculated from the <sup>1</sup>H-broadband-decoupled <sup>13</sup>C spectra by an exponential fit program implemented in the spectrometer software. The relaxation data were extracted from the signal heights. The measurements of the spin–lattice relaxation times were repeated at least five times, those for the NOE factors 10 times, and the average values were used in the analysis. The error in the temperature was estimated to be ±1 °C. Chemical shift values were determined using COSY and HETCOR methods.

## Methodology

**<sup>13</sup>C NMR Relaxation Studies.** The relaxation of <sup>13</sup>C in medium-sized molecules at moderate magnetic fields is usually caused by dipolar interactions with directly bonded protons. When the relaxation times are measured under <sup>1</sup>H decoupling conditions, the cross-relaxation term vanishes, and the intramolecular dipolar longitudinal (spin–lattice) relaxation rate (*R*<sub>1</sub><sup>DD</sup> = 1/*T*<sub>1</sub><sup>DD</sup>)<sub>*i*</sub> for the relaxation of <sup>13</sup>C nucleus *i* by *N*<sub>H</sub> protons *j* is connected to the molecular reorientations by<sup>15–20</sup>

$$\left[ \frac{1}{T_1^{DD}} \right]_i = [1/20]N_H[2\pi D_{ij}]^2[J(\omega_C - \omega_H) + 3J(\omega_C) + 6J(\omega_C + \omega_H)] \quad (1)$$

where the dipolar coupling constant is  $D_{ij} = (\mu_0/4\pi)\gamma_C\gamma_H(\hbar/2\pi)r_{ij}^{-3}$ ,  $\mu_0$  is the permeability of vacuum,  $\gamma_C$  and  $\gamma_H$  are the magnetogyric ratios of the <sup>13</sup>C and <sup>1</sup>H nuclei, respectively, and *r*<sub>*ij*</sub> is the length of the internuclear vector between *i* and *j* (C–H = 1.09 Å). *J*( $\omega$ ) are the spectral densities with  $\omega_C$  and  $\omega_H$  the resonance frequencies of the <sup>13</sup>C and <sup>1</sup>H nuclei, respectively.

**Nuclear Overhauser Effect.** The nuclear Overhauser (NOE) factor  $\eta_i$  of carbon atom *i* relaxed by *N*<sub>H</sub> protons *j* is given by<sup>15–20,27</sup>

$$\eta_i = \gamma_H \sum \sigma_{ij} / [\gamma_C \sum (\rho_{ij} + \rho_i^*)] \quad (2)$$

where Σ is from *j* = 1 to *N*<sub>H</sub>,  $\sigma_{ij}$  is the cross-relaxation rate,  $\rho_{ij}$  is the dipolar relaxation rate, and  $\rho_i^*$  is the leakage term that represents the contribution of all other relaxation mechanisms to the relaxation of a <sup>13</sup>C nucleus *i*, thus reducing the NOE factor. Usually, intermolecular dipolar contributions can be neglected for <sup>13</sup>C nuclei with directly bonded protons. Under <sup>1</sup>H decoupling conditions, the sum of  $\rho_{ij}$  over all *N*<sub>H</sub> interacting protons gives the dipolar spin lattice relaxation rate (*R*<sub>1</sub><sup>DD</sup> = *R*<sub>1</sub><sup>Dipolar</sup> = 1/*T*<sub>1</sub><sup>Dipolar</sup>)<sub>*i*</sub>. The relaxation of <sup>13</sup>C exclusively via intramolecular dipolar interaction implies a leakage term  $\rho_i^* = 0$ . Thus the NOE factor reaches its maximum value and depends only on reorientational molecular dynamics.<sup>15–20,27</sup>

$$\eta_{i,\max} = \gamma_H [6J(\omega_C + \omega_H) - J(\omega_C - \omega_H)] / \gamma_C [J(\omega_C - \omega_H) + 3J(\omega_C) + 6J(\omega_C + \omega_H)] \quad (3)$$

**Spectral Densities.** Assuming isotropic tumbling, the spectral densities can be connected to the effective correlation times,  $\tau_c$ , for reorientation of the corresponding internuclear <sup>13</sup>C–<sup>1</sup>H vectors by

$$J(\omega) = 2\tau_c / [1 + (\omega\tau_c)^2] \quad (4)$$

In theory  $\tau_c$  is the time required for a molecule (i.e., vector connecting the interacting nuclei) to rotate through an angle of one radian; however, in fact, the correlation time is the integral with respect to time from 0 to ∞ of the normalized autocorrelation function<sup>16,19,20</sup> and is actually  $\tau_2$ , the time constant for the exponential decay of the second-rank Legendre polynomial *P*<sub>2</sub>. In the extreme narrowing case (low viscosity solutions—unlike ionic liquids) the product of  $\omega\tau_c$  is much less than unity and *J*( $\omega$ ) = 2 $\tau_c$ .

**Chemical Shift Anisotropy (CSA).** Aromatic <sup>13</sup>C nuclei relax even in moderate magnetic fields partially via the chemical-shift anisotropy (CSA) mechanism. The corresponding longitudinal relaxation rate of <sup>13</sup>C nucleus *i* is given by<sup>15–20</sup>

$$R_1^{\text{CSA}} = [1/15]\gamma_C^2 H_o^2 (\Delta\sigma_i)^2 [1 + (\eta_{\text{CSA}}^2/3)]J(\omega_C) \quad (5)$$

with the magnetic field strength  $H_0$ , the chemical-shift anisotropy  $\Delta\sigma$  for an axially symmetric chemical shift tensor and the asymmetry parameter,  $\eta_{\text{CSA}}$ . The  $[1 + \eta_{\text{CSA}}^2/3]$  term usually represents a correction factor of less than 5% and is therefore ignored.

#### Solution of the Combined Dipolar and NOE Equations.

In the case of ring (aromatic) carbons, it is assumed that dipolar relaxation and chemical shift anisotropy make up the overall relaxation rate:

$$R_1^{\text{total}} = R_1^{\text{Dipolar}} + R_1^{\text{CSA}} \quad (6)$$

The dipolar ( $R_1^{\text{Dipolar}}$ ) and chemical shift anisotropy ( $R_1^{\text{CSA}}$ ) spin–lattice relaxation rates for aromatic carbons may be obtained as follows: (1) the experimental  $T_1$ 's are assumed to be completely dipolar and eq 1 is solved for a pseudorotational correlation time as follows:

$$\tau_c = [10/T_1 N_H (2\pi D_{ij})^2] [(1/[1 + (\omega_C - \omega_H)^2 \tau_c^2]) + (3/[1 + \omega_C^2 \tau_c^2]) + (6/[1 + (\omega_C + \omega_H)^2 \tau_c^2])] \quad (7)$$

Values of  $\tau_c$  were calculated by successive approximations by setting  $\tau_c$  on the right-hand side of eq 7 equal to the previously calculated value. The initial value of  $\tau_c$  was set at 0.01 ns. A constant value of  $\tau_c$  was obtained after approximately five iterations; however, the value after 40 iterations was utilized.

(2) Equations 1 and 3 are combined to form eq 8. The experimental  $T_1$ 's and the pseudorotational correlation times from eq 7 were used in eq 8 to calculate  $\eta_{\text{max}}$ . If these values of  $\eta_{\text{max}}$  were greater than 1.99,  $\eta_{\text{max}}$  was set equal to 1.99.

$$\eta_{\text{max}} = N_H [T_1^{\text{DD}}/20] (\gamma_H/\gamma_C) (2D_{ij})^2 [6J_+ - J_-] \quad (8)$$

where  $J_+ = [2\tau_c/[1 + (\omega_C + \omega_H)^2 \tau_c^2]]$  and  $J_- = [2\tau_c/[1 + (\omega_C - \omega_H)^2 \tau_c^2]]$ .

The corrected ring carbon  $R_1^{\text{Dipolar}}$  is then calculated using the experimental  $T_1$ 's as follows:

$$R_1^{\text{Dipolar}} = (\text{NOE}/\text{NOE}_{\text{max}})/T_1^{\text{total}} \quad (9)$$

The result obtained from eq 9 is then used to solve eq 1 to determine a corrected rotational correlation time ( $\tau_c$ ) for each aromatic carbon. It is then possible to do a repeating set of calculations using the previously established values for  $R_1^{\text{Dipolar}}$  to generate new values for  $\tau_c$ ,  $\eta_{\text{max}}$  and new  $R_1^{\text{Dipolar}}$ . After three cycles, the values of  $\tau_c$  are reasonably well established.

Finally, the aromatic carbon chemical shift anisotropy ( $R_1^{\text{CSA}}$ ) spin–lattice relaxation rates are determined from eq 6. Equation 5 is then used to calculate the chemical shift anisotropy ( $\Delta\sigma$ ) for an axially symmetric chemical-shift tensor.

## Results and Discussion

**Basic Assumptions.** The basic assumption in this analysis is that the maximum value of the  $^{13}\text{C}$  NOE in eq 3 is determined by the dipolar rotational correlation time obtained from the measured relaxation rate. This assumption is based on the validity of eq 3, the derivation of which is outlined in numerous references.<sup>15–20,27</sup>

**Sources of Error.** Sources of error include the possibility of biexponential behavior and the use of an isotropic model to describe anisotropic motion. At present, there appear to be no examples of biexponential behavior in the literature as far as viscous solutions of this type are concerned. Despite its inherent assumptions, the isotropic model has proved to be reasonably

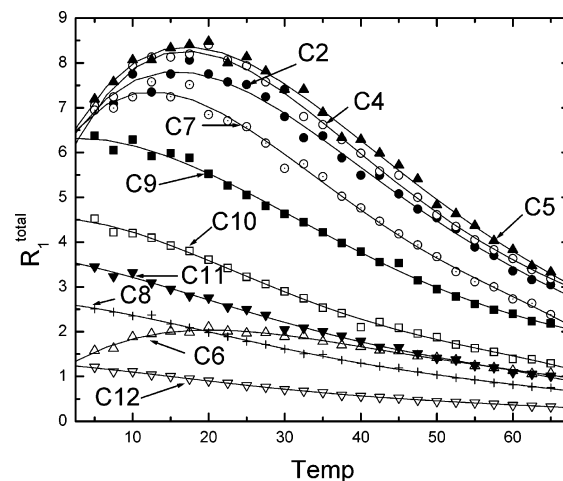


**Figure 3.**  $^{13}\text{C}$  Total spin–lattice relaxation rates ( $\text{s}^{-1}$ ) for [EMIM]- $\text{BSO}_3$  ionic liquid vs temperature. Imidazolium ring  $^{13}\text{C}$ 's: C2, 139.9 ppm (●); C4, 124.0 ppm (○); C5, 122.5 ppm (▲). Ring methyl  $^{13}\text{C}$ : C6, 35.9 ppm (△). Ring methylene  $^{13}\text{C}$ : C7, 44.6 ppm (○). Terminal methyl  $^{13}\text{C}$ : C8, 15.6 ppm (+). Butanesulfonate  $^{13}\text{C}$ 's:  $\text{SO}_3$  methylene  $^{13}\text{C}$ , C9, 51.9 ppm (■); methylene  $^{13}\text{C}$ , C10, 27.9 ppm (□), methylene  $^{13}\text{C}$ : C11–22.1 ppm (▼) and terminal methyl  $^{13}\text{C}$ : C12–13.9 ppm (▽).

successful in describing a wide range of viscous solutions and providing useful physical information concerning these systems.<sup>22,29–31</sup>

Other easily detected problems include scalar relaxation and chemical exchange.<sup>15–17,20,22</sup> Scalar relaxation will not be a factor in this study as it arises only when (a) the Larmor frequencies are similar (carbon bonded to bromine) or when a slowly relaxing nucleus is bonded to a fast relaxing nucleus (carbon bonded to aluminum). Chemical exchange is generally present when observed NMR peaks are seen to coalesce with increasing temperature as the exchange rate between species is faster than the NMR time scale. Temperature studies of [EMIM]BSO<sub>3</sub> fail to indicate the presence of any of the above relaxation mechanisms.

There is also the question of molecular mobility using the isotropic model. A detailed analysis of [BMIM]PF<sub>6</sub> and [MNIM]PF<sub>6</sub> ionic liquids has provided a reasonable description of molecular mobility in each case.<sup>29–31</sup> Such analyses are supported by a molecular dynamics study of [BMIM]PF<sub>6</sub>.<sup>35</sup> A theoretical study<sup>36</sup> of homonuclear NOE's as probes of molecular mobility, concluded that in general, NOE's are insensitive to internal mobility and depend solely on overall molecular mobility. The extension of this conclusion to heteronuclear systems is supported to a limited extent by the correlation between diffusion coefficients and  $^{13}\text{C}$  relaxation rates in viscous solutions.<sup>24–26</sup>

#### Comparison of $^{13}\text{C}$ Chemical Shifts and Relaxation Times.

The presence of carbon nuclei in both the [EMIM] cation and BSO<sub>3</sub> anion allows for a correlation of cationic and anionic molecular mobility on the same NMR time scale. Figure 2 contains the  $^{13}\text{C}$  chemical shifts of the [EMIM] cation and BSO<sub>3</sub> anion relative to TMS. The [EMIM] imidazolium ring  $^{13}\text{C}$  chemical shift values are similar to those obtained previously for the [BMIM] and [MNIM] cations.

**$^{13}\text{C}$  Total Relaxation Rates for Both [EMIM] Cation and Butanesulfonate Anion.** Figure 3 contains the  $^{13}\text{C}$  total spin relaxation rates for imidazolium and BSO<sub>3</sub> carbons in the [EMIM]BSO<sub>3</sub> ionic liquid. The imidazolium ring carbons (C2,C4,C5), the methyl and methylene carbons attached directly to the imidazolium ring (C6,C7) have a maximum ( $=T_1$



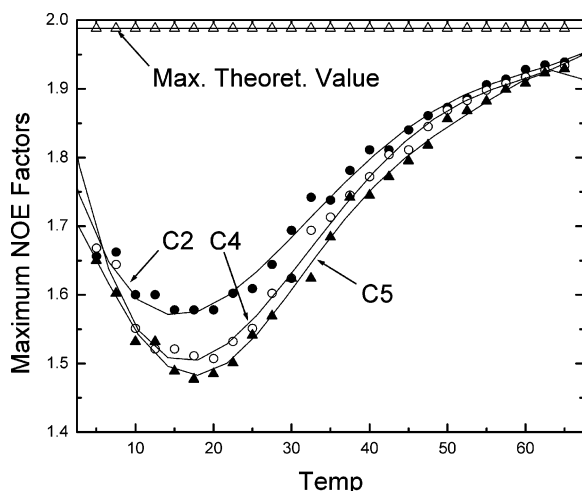


**Figure 4.** Corrected maximum  $^{13}\text{C}$  NOE factors and total spin–lattice relaxation times ( $T_1$ 's). For [MNIM]PF<sub>6</sub> ionic liquid vs temperature: (●) imidazolium ring C2 carbon; (○) imidazolium ring C4 and (▲) C5 carbons; (Δ) theoretical NOE  $^{13}\text{C}$  maximum of 1.988.

minimum) in the region 15–20 °C. The terminal ring methyl (C8) and the butyl sulfate carbons (C9,C10,C11,C12) have maxima at less than 0 °C. These results indicate that the butyl carbons and the methyl carbon in the ring ethyl group are less constrained than those attached directly to the imidazolium ring. Similar results have been obtained for the [BMIM]PF<sub>6</sub> and [MNIM]PF<sub>6</sub> ionic liquids.<sup>30,31</sup>

**Corrected Maximum NOE Factors.** The corrections to the maximum NOE factors in the [EMIM]BSO<sub>3</sub> ionic liquid are shown in Figure 4. Although CSA effects appear for the ring methyl and adjacent methylene carbons (discussed in a later section), these methylene carbons do not require a correction to the maximum NOE factor.

**Cationic and Anionic Rotational Correlation Times.** The initial rotational correlation times ( $\tau_c$ ) are determined using eqs 1 (assuming complete dipolar relaxation) 7, 8, 9, 1 and 6 sequentially as outlined in the methodology section. The corrected rotational correlation times (picoseconds) for the imidazolium ring carbons and other remaining cationic and anionic carbons are shown in Figure 5. The corrected (final) rotational correlation times are shorter than the initial rotational correlation times, and the total relaxation rate is now separated into both dipolar relaxation and a second contribution (chemical shift anisotropy). Correction of the imidazolium ring carbon NOE's results in a correlation time maximum at 40–50 °C, a shift of ca. 25 °C from the  $R_1$  maximum ( $=1/T_1$  minimum) for these same carbons. At the same time, the imidazolium ring methyl group (C6) also has a correlation time maximum at 40–50 °C whereas the imidazolium ring methylene group (C7) has a maximum at a slightly lower temperature of ca. 35 °C.

The imidazolium ring carbon C2 correlation times ( $\tau_c$ ) maximum at  $\approx 45$  °C lies between correlation time maxima of 37 and 52 °C for the imidazolium C2 carbons in [BMIM]PF<sub>6</sub> and [MNIM]PF<sub>6</sub> ionic liquids.<sup>30,31</sup> The results for the methyl and methylene ring carbons are similar to those obtained for the [BMIM]PF<sub>6</sub> and [MNIM]PF<sub>6</sub> ionic liquids.<sup>30,31</sup>

**NMR Correlation Times and Viscosity.** In classical mechanics, the correlation time,  $\tau_c$ , of spherical particle undergoing isotropic rotation is given by the SED equation:

$$\tau_c = 4\pi a^3 \eta / 3kT = V\eta / kT \quad (10)$$

For those correlation times determined by NMR, the relationship

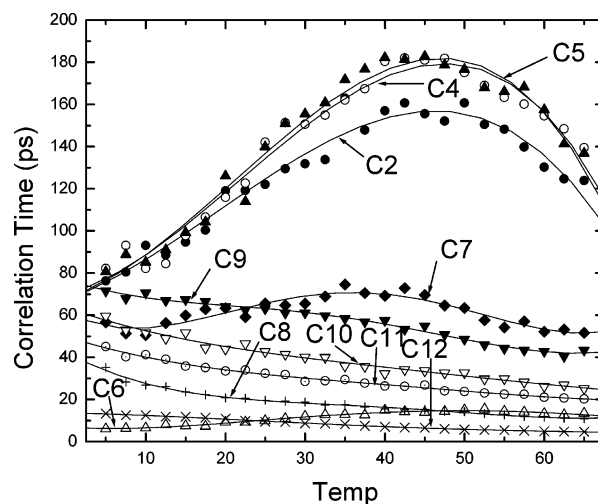


**Figure 5.**  $^{13}\text{C}$  Correlation times (ps) for [EMIM]BSO<sub>3</sub> ionic liquid vs temperature. Imidazolium ring  $^{13}\text{C}$ 's: C2, 139.9 ppm (●); C4, 124.0 ppm (○); C5, 122.5 ppm (▲). Ring methyl  $^{13}\text{C}$ : C6, 35.9 ppm (Δ). Ring methylene  $^{13}\text{C}$ : C7, 44.6 ppm (◆). Terminal methyl  $^{13}\text{C}$ : C8, 15.6 ppm (+). Butanesulfonate  $^{13}\text{C}$ 's: SO<sub>3</sub> methylene  $^{13}\text{C}$ , C9, 51.9 ppm (▼); methylene  $^{13}\text{C}$ , C10, 27.9 ppm (▽); methylene  $^{13}\text{C}$ , C11, 22.1 ppm (×); terminal methyl  $^{13}\text{C}$ , C12, 13.9 ppm (×).

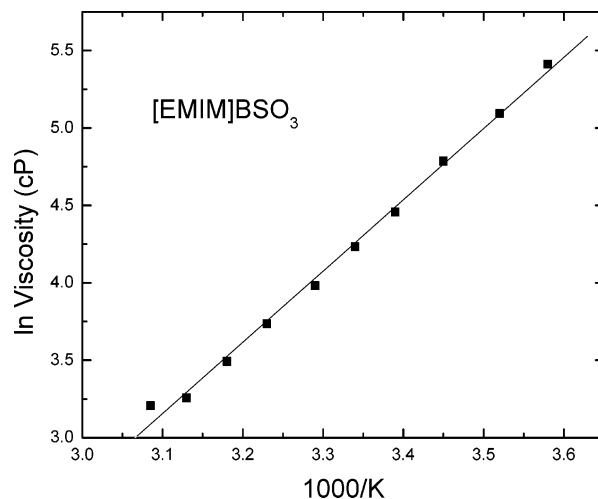


**Figure 6.** ln viscosity (cP) of [EMIM]BSO<sub>3</sub> ionic liquid vs 1000/K.  $E_a = 9.14$  kcal/mol from 279.6 to 324.1 K.

between  $\tau_c$  and temperature in the viscosity-dependent region is given by<sup>37</sup>

$$\tau_c = \tau_o + \eta \tau_{\text{red}} / T \quad (11)$$

where  $\tau_{\text{red}} = V/k$ . The values of  $a$ , the hydrodynamic radius, obtained from this type of analysis are typically too small<sup>38–42</sup> and are often corrected using a nonspherical rotational model.<sup>37</sup>

Figure 6 is a ln plot of the measured viscosity of the [EMIM]BSO<sub>3</sub> ionic liquid vs 1000/K. There is no evidence of any discontinuities between 6.6 and 51.1 °C, although the viscosity tends to level off at the high-temperature end. The calculated activation energy is 9.14 kcal/mol. The measured viscosity data were fitted to a polynomial as a function of temperature ( $R^2 = 0.999$ ) and used to generate viscosity values at temperatures identical to those used in the NMR relaxation measurements.

Figure 7 contains a plot of [EMIM] ring carbon (C2,C4,C5) NMR correlation times vs viscosity/K for the [EMIM]BSO<sub>3</sub> ionic liquid. A similar plot was obtained for the more viscous ionic liquid, [MNIM]PF<sub>6</sub>.<sup>31</sup> As is the case with [MNIM]PF<sub>6</sub>, [EMIM]BSO<sub>3</sub> undergoes several phase changes and the only

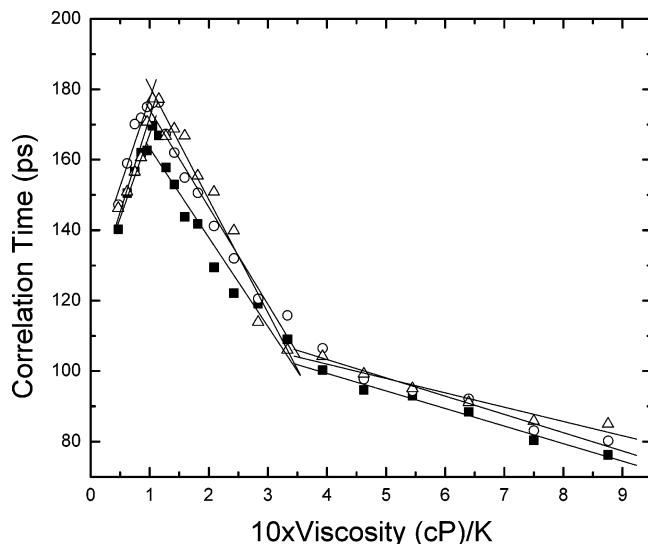


**Figure 7.** Correlation time (ps) for C2 (■), C4 (○) and C5 (△) vs viscosity/K (cP/K) for [EMIM] in [EMIM]BSO<sub>3</sub>. From left to right, temperature ranges include 328–308, 308–293, and 293–278 K.

region where the slope is positive is at the higher temperatures between 35 and 55 °C. The slopes in this temperature range are 476, 496, and 536 (ps K)/cP that translate into  $a$  values of 1.16, 1.18 and 1.21 Å (C2,C4,C5) for the 1-ethyl-3-methylimidazolium cation. The average  $a$  value (radius) of 1.18 Å may be compared with an  $a$  value of 1.15 Å obtained for the 1-ethyl-3-methylimidazolium cation in a 1-ethyl-3-methylimidazolium chloride–ethyl aluminum chloride melt.<sup>12</sup> However, both  $a$  values of 1.15 and 1.18 Å are less than 50% of the [EMIM] radius obtained from gas phase calculations (Figure 1). However, these unjustifiably small values of cationic radii can be “changed” to more reasonable values using “frictional” correction factors.

**Correction of SED  $a$  Values.** The classical model of a sphere rotating in a continuous medium may be adjusted to account for the results obtained from eq 10 using either the Gierer–Wirtz<sup>43</sup> or Hu–Zwanzig<sup>44</sup> models. The Gierer–Wirtz model<sup>43</sup> introduces a rotational microviscosity factor  $f$  whose radius ratio dependence is given by

$$f = [6(a_s/a) + (1 + a_s/a)^{-3}]^{-1} \quad (12)$$

where  $a_s$  = solvent and the functional dependence of  $f$  upon  $a_s/a$  results in only a minor correction when the solvent molecule is very small or the solute molecule is very large. For neat and other liquids where the solute and solvents sizes are similar,  $f$  is 0.16. In cases where the solvent molecule is very large compared to the solute (10:1),  $f$  may be as small as 0.02.

The Gierer–Wirtz model<sup>43</sup> is an adjustment for spherical molecules that corrects for the observation that molecular rotational friction coefficients are less than the Stokes value of  $8\pi\eta a^3$ . The Gierer–Wirtz model is adequate for describing rotation about the symmetry axis; however, rotation of the symmetry axis requires displacement of solvent molecules, introducing viscous drag even in the slip limit.<sup>37</sup>

The classical “stick” (SED) frictional model does not accurately represent the [EMIM]BSO<sub>3</sub> ionic liquid as evidenced by the unrealistic  $a$  value (radius) of 1.18 Å for the 1-methyl-3-nonylimidazolium cation. The calculated gas-phase volumes of the 1-ethyl-3-methylimidazolium cation and the BSO<sub>3</sub> anion (Figure 1) are similar, being approximately 150 and 155 Å<sup>3</sup>, respectively. The calculated gas-phase value of the  $a$

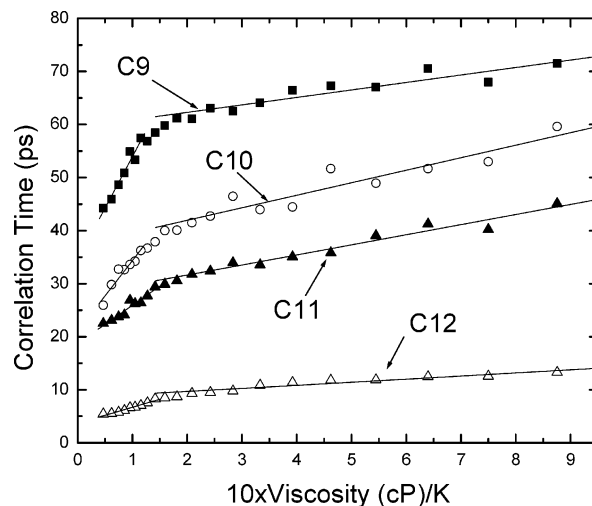


**Figure 8.** Correlation time (ps) for butyl carbons in BSO<sub>3</sub> in [EMIM]BSO<sub>3</sub> vs viscosity/K (cP/K): C9 (■); C10 (○); C11 (▲); C12 (△). From left to right, temperature ranges include approximately 328–303 K and 303–278 K.

parameter for the 1-ethyl-3-methyl-imidazolium cation is  $3.30 \pm 0.30$  Å that would require a correction factor ( $f$ ) of 0.046. The calculated gas-phase value of  $a$  for the BSO<sub>3</sub> anion is  $3.33 \pm 0.33$  Å, resulting in an  $a_s/a$  ratio of approximately 1 and a correction factor ( $f$ ) of 0.16.<sup>43</sup> This results in an increase (correction) of the cation  $a$  parameter from 1.18 to 2.17 Å or 66% of the expected value (3.30 Å).<sup>43</sup>

Despite the similarities in molecular volumes, the shape of the [EMIM] cation and BSO<sub>3</sub> anion are somewhat different. In fact, ionic liquids are seldom spherical and often may be regarded as prolate (cigar-shaped;  $a = b < c$ ) or oblate (pancake-shaped;  $a < b = c$ ) spheroids whose rotational motion is anisotropic.<sup>37,44</sup> The Hu–Zwanzig<sup>44</sup> slipping boundary model accounts for the viscous drag frictional coefficient in both the prolate and oblate spheroid models over a range of  $a/c$  values. In view of the ethyl and methyl imidazolium side chains in the [EMIM]BSO<sub>3</sub> ionic liquid (Figure 1), it seems reasonable to assume that the [EMIM] cation may be considered as a prolate (cigar-shaped) spheroid undergoing anisotropic rotational motion. One can only estimate  $a$ ,  $b$  and  $c$  ( $a = b < c$ ) axis values for the [EMIM] cation. The distance from the methyl group to the end of the ethyl group can be estimated at approximately  $7.5 \pm 1$  Å. The other axes are estimated at  $2.2 \pm 0.5$  Å. These estimated values result in a  $f_{\text{slip}}$  correction factor of 0.12 that is a mild improvement over the correction factor of 0.16 obtained from the Gierer–Wirtz<sup>43</sup> model. This translates to a corrected spherical (SED)  $a$  parameter (radius) of 2.39 Å or 72% of the theoretical gas phase  $a$  parameter (3.30 Å) and is satisfactory, considering the various approximations used herein.<sup>44</sup>

**Anion–Viscosity Relationships.** Figure 8 contains a plot of the butyl carbon BSO<sub>3</sub> (C9,C10,C11,C12) NMR correlation times vs viscosity/K for the [EMIM]BSO<sub>3</sub> ionic liquid. Unlike the [EMIM] cation in [EMIM]BSO<sub>3</sub>, one observes only a single phase for the BSO<sub>3</sub> anion change in the vicinity of 25–35 °C. Furthermore, there are no additional phase changes observed between 5 and 30 °C for the BSO<sub>3</sub> anion. The slopes in the upper temperature range 30–55 °C are 194, 133, 72 and 30 (ps K)/cP that translate into  $a$  values (radii) of 0.86, 0.76, 0.62 and 0.46 Å (C9,C10,C11,C12) for the butanesulfonate anion. Although chemical shift anisotropy (CSA) is present in C9, C10 and C11 (discussed in the following section), extension of the cation  $a$  parameter (radius) analysis to the BSO<sub>3</sub> anion is highly questionable at this point. This is further supported by the fact

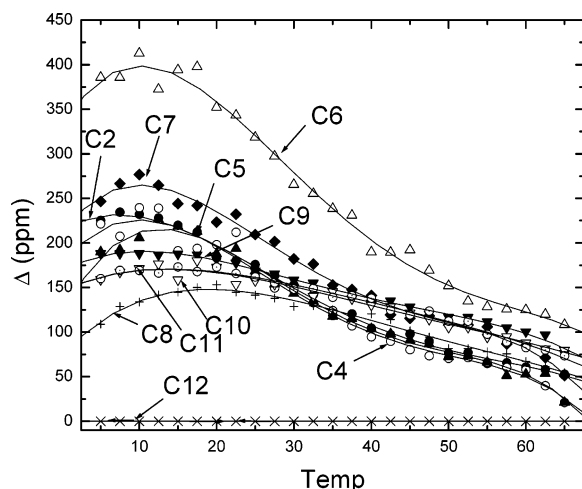


**Figure 9.**  $^{13}\text{C}$  CSA ( $\Delta\sigma$ ) for [EMIM]BSO<sub>3</sub> ionic liquid vs temperature. Imidazolium ring  $^{13}\text{C}$ 's: C2, 139.9 ppm (●); C4, 124.0 ppm (○); C5, 122.5 ppm (▲). Ring methyl  $^{13}\text{C}$ : C6, 35.9 ppm (△). Ring methylene  $^{13}\text{C}$ : C7, 44.6 ppm (◆). Terminal methyl  $^{13}\text{C}$ : C8, 15.6 ppm (+). Butanesulfonate  $^{13}\text{C}$ 's: SO<sub>3</sub> methylene  $^{13}\text{C}$ , C9, 51.9 ppm (▼); methylene  $^{13}\text{C}$ , C10, 27.9 ppm (▽); methylene  $^{13}\text{C}$ , C11, 22.1 ppm (⊙); terminal methyl  $^{13}\text{C}$ , C12, 13.9 ppm (×).

that slopes of the plot in Figure 8 are even smaller (5.8–23.6 (ps K)/cP) at the lower temperatures (5–30°) and yield extremely small values of  $a$  for the butanesulfate anion (0.27–0.42 Å).

**Chemical Shift Anisotropy (CSA).** The chemical shift anisotropy (eq 5) is typically defined as

$$\Delta\sigma = |\sigma_{\parallel} - \sigma_{\perp}| = \sigma_{zz} - (\sigma_{xx} + \sigma_{yy})/2 \quad (13)$$

with  $|\sigma_{zz}| \geq |\sigma_{yy}| \geq |\sigma_{xx}|$ . The asymmetry parameter,  $\eta_{\text{CSA}}$ , is generally ignored (as mentioned previously) in chemical shift anisotropy analysis as it would normally result in less than a 5–10% correction as shown in solid state<sup>45</sup> isotropic studies. Using the convention outlined for eq 9, the asymmetry factor is given by<sup>15–20,45</sup>

$$\eta_{\text{CSA}} = (3/2)(\sigma_{xx} - \sigma_{yy})/\Delta\sigma \quad (14)$$

Figure 9 contains a plot of  $^{13}\text{C}$  CSA vs temperature for the [EMIM] cation and the butanesulfonate anion in the [EMIM]-BSO<sub>3</sub> ionic liquid. In previous studies of [BMIM]PF<sub>6</sub> and [MNIM]PF<sub>6</sub>, CSA was observed for the imidazolium carbons and those carbons immediately adjacent to the imidazolium ring. In the case of the [EMIM]BSO<sub>3</sub> ionic liquid, one observes CSA for the ring methyl and ethyl carbons and for the three carbons nearest to the sulfonate group. Only the terminal carbon in the butyl group fails to exhibit CSA dependency. In previous studies of [BMIM]PF<sub>6</sub> and [MNIM]PF<sub>6</sub> ionic liquids, CSA was present only in either the ring carbons or those carbons immediately adjacent to the imidazolium ring. The [EMIM]BSO<sub>3</sub> ionic liquid exhibits CSA in all of the imidazolium carbons and all butyl carbons with the exception of the terminal methyl carbon. As was observed for the [BMIM]PF<sub>6</sub> and [MNIM]PF<sub>6</sub> ionic liquids, the imidazolium methyl carbon (C6) has the highest  $\Delta\sigma$  value (Figure 9) over the temperature range 5–65 °C. The average  $\Delta\sigma$  values for the imidazolium ring and butanesulfonate carbons are C2–136, C4–130, C5–139, C6–251, C7–147, C8–113, C9–167, C10–135 and C11–136 ppm. Unlike the other carbons in both the cation and anion, the C12 carbon displays only dipolar relaxation.

The  $\Delta\sigma$  values for the ring carbons are similar to those in the [BMIM] and [MNIM] imidazolium cations over similar temperature ranges. Maximum ring carbon values of  $\Delta\sigma$  for [EMIM]BSO<sub>3</sub> are reached in the range 5–15 °C, as are those of the butyl side chain carbons. The  $\Delta\sigma$  values for the ring C2, C4 and C5 carbons reach maximum values of 226, 239 and 226 ppm at 10 °C and then decrease to lower values at both higher and lower temperatures. The averaged  $\Delta\sigma$  values for C2, C4 and C5 over the entire temperature range are 136, 130 and 139 ppm. The average  $\Delta\sigma$  values for the three imidazolium ring carbons (136, 130 and 139 ppm) may be compared with isotropic values of 159, 157 and 121 ppm for pyrimidine in liquid crystal solutions.<sup>46</sup>

There is the unresolved question of temperature dependence;<sup>16</sup> however, [EMIM]BSO<sub>3</sub>, [BMIM]PF<sub>6</sub> and [MNIM]PF<sub>6</sub> are systems of ion pairs that have considerable equilibrium characteristics. Of considerable importance is the recent mass spectrometry study that directly establishes the ability of ionic liquids to form a variety of aggregates, a fact that adds credence to the equilibrium picture of ionic liquids.<sup>13</sup> Even in static systems, relatively small changes in the position of a single hydrogen atom can result in major shifts in the tensorial shieldings.<sup>47</sup> It has also been reported that the isotropic average of the shielding tensor is closely related to the isotropic shift in liquids, showing only little dependence on packing in the solid state.<sup>48</sup> In view of these observations, perhaps the temperature dependence of  $\Delta\sigma$  in [BMIM]PF<sub>6</sub> and [MNIM]PF<sub>6</sub> ionic liquids is to be expected.

**Conclusions.** The recent report<sup>13</sup> of aggregation in ionic liquids complements this NMR and viscosity study in several ways. The  $^{13}\text{C}$  NMR correlation times vs viscosity/K plots (Figures 7 and 8) indicate several phase changes for the [EMIM] cation (20 and 35 °C) and at least one phase change (approximately 30 °C) for the BSO<sub>3</sub> anion. The methyl ring carbon (C6) undergoes relatively free “rotation” (low picosecond range) and yet requires that chemical shift anisotropy plays a major role in addition to dipolar relaxation. This result is consistent with the likely aggregation of the [EMIM]BSO<sub>3</sub> ionic liquid. A similar conclusion may be reached for the [BMIM]PF<sub>6</sub> and [MNIM]PF<sub>6</sub> ionic liquids.<sup>30,31</sup>

**Acknowledgment.** W.R.C. thanks the National Research Council for a Summer Research Faculty Fellowship and Professors Andreas Dölle and Manfred Zeidler for many fruitful discussions.

## References and Notes

- (1) Hussey, C. L. *Adv. Molten Salt Chem.*, **1983**, 5, 185–230.
- (2) Wasserscheid, P.; Keim, W. *Angew. Chem. (Int. Ed.)* **2000**, 39, 3772–3789.
- (3) Welton, T. *Chem. Rev.* **1999**, 99, 2071–2083.
- (4) Wilkes, J. S. *Green Chem.* **2002**, 4, 73–80.
- (5) Wasserscheid, P.; Welton, T. *Ionic Liquids in Synthesis*; John Wiley: New York, 2002.
- (6) Letcher, T. M.; Marciniak, A.; Marciniak, M.; Domanska, U. *J. Chem. Eng. Data* **2005**, 50, 1294–1298.
- (7) Koelle, P.; Dronsowski, R. *Inorg. Chem.* **2004**, 43, 2803–2809.
- (8) Wasserscheid, P.; van Hal, R.; Boesmann, A.; Esser, J.; Jess, A. New Ionic Liquids Based on Alkyl sulfate and Alkyl Oligoether Sulfate Anions: Synthesis and Applications. In *Ionic Liquids as Clean Solvents*; Rogers, R. D., Seddon, K. R., Eds.; ACS Symposium Series No. 856; American Chemical Society: Washington, DC, 2003; pp 57–69.
- (9) Holbrey, J. D.; Reichert, W. M.; Swatoski, R. P.; Broker, G. A.; Pitner, W. R.; Seddon, K. R.; Rogers, R. D. *Green Chem.* **2002**, 4, 407–413.
- (10) Ogihara, W.; Yoshizawa, M.; Ohno, H. *Chem. Lett.* **2002**, 880–881.
- (11) Tatumi, R.; Fujihara, H. *Chem. Commun.* **2005**, 83–85.

- (12) Gui, J.; Ban, H.; Cong, X.; Zhang, X.; Hu, Z.; Sun, Z. *J. Mol. Catal.* **2005**, *225*, 27–31.
- (13) Dorbritz, S.; Ruth, W.; Kragl, U. *Adv. Synth. Catal.* **2005**, *347*, 1273–1279.
- (14) Consorti, C. S.; Suarez, P. A. Z.; de Souza, R. F.; Burrow, R. A.; Farrar, D. H.; Lough, A. J.; Loh, W.; de Silva, L. H. M.; Dupont, J. *J. Phys. Chem. B* **2005**, *109*, 4341–4349.
- (15) Abragam, A. *Principles of Nuclear Magnetism*; Oxford University Press: Oxford, U.K., 1961; Chapter 8.
- (16) Farrar, T. C.; Becker, E. D. *Pulse and Fourier Transform NMR. Introduction to Theory and Methods*; Academic Press: New York, 1971.
- (17) Spiess, H. W. In *NMR: Basic Principles and Progress*; Diehl, P., Fluck, E., Kosfeld, R., Eds.; Springer-Verlag: Berlin, 1978; Vol. 15, p 55.
- (18) Canet, D.; Robert, J. B. In *NMR: Basic Principles and Progress*; Diehl, P., Fluck, E., Gunther, H., Kosfeld, R., Seelig, J., Eds.; Springer-Verlag: Berlin, 1990; Vol. 25, p 46.
- (19) McConnell, J. *Nuclear Magnetic Relaxation in Liquids*; Cambridge University Press: Cambridge, U.K., 1987.
- (20) Canet, D. *Nuclear Magnetic Resonance: Concepts and Methods*; John Wiley & Sons: New York, 1996.
- (21) Halle, B.; Wennerstrom, H. *J. Magn. Reson.* **1981**, *44*, 89.
- (22) Carper, W. R. *Concepts Magn. Reson.* **1999**, *11*, 51.
- (23) Keller, C. E.; Carper, W. R. *J. Magn. Reson.* **1994**, *A110*, 125.
- (24) Larive, C. K.; Lin, M.; Piersma, B. J.; Carper, W. R. *J. Phys. Chem.* **1995**, *99*, 12409–12412.
- (25) Carper, W. R.; Mains, G. J.; Piersma, B. J.; Mansfield, S. L.; Larive, C. K. *J. Phys. Chem.* **1996**, *100*, 4724–4728.
- (26) Larive, C. K.; Lin, M.; Kinnear, B. S.; Piersma, B. J.; Keller, C. E.; Carper, W. R. *J. Phys. Chem.* **1998**, *102B*, 1717.
- (27) Neuhaus D.; Williamson M. P. *The Nuclear Overhauser Effect in Structural and Conformational Analysis*; Wiley-VCH Press: New York, 2000.
- (28) Dölle, A. *J. Phys. Chem. A* **2002**, *106*, 11683.
- (29) Antony, J. H.; Mertens, D.; Dölle, A.; Wasserscheid, P.; Carper, W. R. *ChemPhysChem* **2003**, *4*, 588.
- (30) Carper, W. R.; Wahlbeck, P. G.; Dölle, A. *J. Phys. Chem. A* **2004**, *108*, 6096–6099.
- (31) Antony, J. H.; Dölle, A.; Mertens, D.; Wasserscheid, P.; Carper, W. R.; Wahlbeck, P. G. *J. Phys. Chem. A* **2005**, *109*, 6676–6682.
- (32) Frisch, M. J.; Trucks, G. W.; Schlegel, H. B.; Scuseria, G. E.; Robb, M. A.; Cheeseman, J. R.; Zakrzewski, V. G.; Montgomery, J. A., Jr.; Stratmann, R. E.; Burant, J. C.; Dapprich, S.; Millam, J. M.; Daniels, A. D.; Kudin, K. N.; Strain, M. C.; Farkas, O.; Tomasi, J.; Barone, V.; Cossi, M.; Cammi, R.; Mennucci, B.; Pomelli, C.; Adamo, C.; Clifford, S.; Ochterski, J.; Petersson, G. A.; Ayala, P. Y.; Cui, Q.; Morokuma, K.; Malick, D. K.; Rabuck, A. D.; Raghavachari, K.; Foresman, J. B.; Cioslowski, J.; Ortiz, J. V.; Baboul, J. G.; Stefanov, B. B.; Liu, G.; Liashenko, A.; Piskorz, P.; Komari, I.; Gomperts, R.; Martin, R. L.; Fox, D. J.; Keith, T.; Al-Laham, M. A.; Peng, C. Y.; Nannayakkara, A.; Challacombe, M.; Gill, P. M. W.; Johnson, B.; Chen, W.; Wong, M. W.; Andres, J. L.; Gonzalez, C.; Head-Gordon, M.; Replogle, E. S.; Pople, J. A. *Gaussian 98*, revision A.9; Gaussian, Inc.: Pittsburgh, PA, 1998.
- (33) Bondi, A. *J. Phys. Chem.* **1964**, *68*, 441–451.
- (34) Meng, Z.; Dölle, A.; Carper, W. R. *J. Mol. Struct. (THEOCHEM)* **2002**, *585*, 119–128.
- (35) Antony, J. H.; Mertens, D.; Breitenstein, T.; Dölle, A.; Wasserscheid, P.; Carper, W. R. *Pure Appl. Chem.* **2004**, *4*, 255.
- (36) Werbelow, L. *J. Am. Chem. Soc.* **1974**, *96*, 4747–4749.
- (37) Boere, R. T.; Kidd, R. G. In *Annual Reports on NMR Spectroscopy*; Webb, G. A., Ed.; Academic Press: New York, 1982; Vol. 13, p 319.
- (38) Mitchell, R. W.; Eisner, J. *J. Chem. Phys.* **1960**, *33*, 86.
- (39) Mitchell, R. W.; Eisner, J. *J. Chem. Phys.* **1961**, *34*, 651.
- (40) Waylischen, R. E.; Pettitt, B. A.; Danchura, W. *Can J. Chem.* **1977**, *55*, 3602.
- (41) Kivelson, D.; Kivelson, M. G.; Oppenheim, I. *J. Chem. Phys.* **1970**, *52*, 1810.
- (42) Tyrrell, H. J. V.; Harris, K. R. *Diffusion in Liquids*; Butterworth: London, U.K., 1984.
- (43) Gierer, A.; Wirtz, K. *Z. Naturforsch.* **1953**, *8A*, 522–532.
- (44) Hu, C. M.; Zwanzig, R. *J. Chem. Phys.* **1974**, *60*, 4354–4357.
- (45) Mehring, M. In *High-Resolution NMR Spectroscopy in Solids*; Diehl, P., Fluck, E., Kosfeld, R., Eds.; NMR—Basic Principles and Progress; Springer-Verlag: Berlin, Heidelberg, New York; 1976; Vol 11, p 167.
- (46) Parhami, P.; Fung, B. M. *J. Am. Chem. Soc.* **1985**, *107*, 7304.
- (47) Beeler, A. J.; Orendt, A. M.; Grant, D. M.; Cutts, P. W.; Milchl, J.; Zilm, K. W.; Downing, J. W.; Facelli, J. C.; Schindler, M. S.; Kutzelnigg, W. *J. Am. Chem. Soc.* **1984**, *106*, 7672.
- (48) Gay, I. D.; Young, G. B. *Organometallics* **1996**, *15*, 2264–2269.